The effect of salt and site-directed mutations on the iron(III)-binding site of human serum transferrin as probed by EPR spectroscopy

John K. GRADY,* Anne B. MASON,† Robert C. WOODWORTH† and N. Dennis CHASTEEN*‡

*Department of Chemistry, Parsons Hall, University of New Hampshire, Durham, NH 03824-3598, U.S.A., and †Department of Biochemistry, University of Vermont College of Medicine, Burlington, VT 05405-0068, U.S.A.

The effects of site-directed mutation and salt on the iron(III)-binding site of the recombinant half-molecule of the N-terminal lobe (hTf/2N) of human transferrin was studied by EPR spectroscopy. Changes were observed in the EPR spectra of all variants investigated (D63S, D63C, G65R, K206Q, H207E, H249E, H249Q, K296E and K296Q) compared with that of the wild-type protein. The most pronounced changes in the metal site were caused by replacement of the coordinating residues, Asp-63 and His-249, and the non-coordinating residue Lys-296, which is located in the hinge region of the iron-binding cleft. The EPR spectral changes from replacement of other non-coordinating residues were more subtle, indicating small changes in Fe^{3+} coordination to the protein. The EPR spectrum of variant G65R suggests that it adopts two distinct conformations in solution, one in which the two domains forming the iron-binding cleft are closed and one in which they are open; in the latter instance Asp-63 is no longer coordinated to the Fe^{3+}. Chloride-binding studies on hTf/2N, K206Q, H207E, K296Q and K296E showed similar binding isotherms, indicating that none of the hinge region residues replaced, i.e. Lys-206, His-207 or Lys-296, are the sites of chloride binding. The results show that the coordination environment of the Fe^{3+} is sensitive to structural changes from site-directed mutation of both remote and co-ordinated residues and also to chloride-binding and ionic strength effects.

INTRODUCTION

The transferrins, human serum transferrin (hTf), ovotransferrin (OTf) and lactoferrin (LTf), are a family of iron-complexation and transport proteins found in the blood and body fluids of a wide variety of species [1,2]. X-ray crystallography has shown that the single polypeptide chain of $M_r \sim 80000$ consists of N- and C-lobes each composed of two domains [3–6]. Each lobe binds one Fe^{3+} ion cooperatively with the physiological synergistic anion carbonate, but other suitable anions can function in place of carbonate [3,7–9]. The two iron-binding sites are structurally similar but exhibit different kinetic and thermodynamic properties [10–15].

The coordination of the synergistic anion and subsequent binding of iron is associated with a conformational change from open to closed, in which the binding cleft is formed by closure of the N1 domain over the N2 domain [3,4]. The N1 domain contributes an aspartate residue (Asp-63) as an Fe^{3+} ligand with histidine (His-249) and tyrosine (Tyr-95) ligands coming from the interdomain hinging strands [3,6] (hTf numbering). A tyrosine ligand (Tyr-188) is contributed from the N2 domain. The coordination sphere is completed by the bidentate chelation of the carbonate anion, which is hydrogen-bonded to several residues (Arg-124, Thr-120, Ala-126 and Gly-127) in the binding cleft, to give a six-coordinate Fe^{3+} complex [3,5,6,16,17].

In addition to the synergistic anion carbonate, a number of other anions such as chloride and phosphate have been shown to bind non-synergistically to hTf and to affect its spectroscopic and iron-binding properties [12,18–26]. Early investigations of the stoichiometry of binding of chloride and other anions with various transferrins suggested that two anions are bound per lobe with strong pairwise cooperativity [18,27]. Other experiments have shown that the rate of iron release to the chelator 3,4-LICAMS [*N*,*N*′,*N*″-tris(5-sulpho-2,3-dihydroxybenzoyl)-1,5,10-triazadecane] depends on the ionic strength of the solution, with the rate approaching zero as the ionic strength of the solution approaches zero [28], an observation suggesting that non-synergistic anion binding and/or a sufficiently high ionic strength is required for iron release from the protein to occur. Binding of transferrin to its receptor and chloride binding to the protein have been shown to be independent of one another, but the binding of chloride is required in order for iron release from the receptor-bound protein to occur [26]. While the identity of the binding sites on transferrin for chloride or for the receptor are as yet unknown, it has been suggested that one or both of these sites may be located on the hinging strands connecting the two domains, thus facilitating the change between the closed and open conformations during iron release from the receptor-bound protein [26].

Recent studies of the recombinant N-lobe half-molecule of human serum transferrin (hTf/2N) and a number of site-directed mutants listed in Table 1 have allowed measurement of the effect of point mutations on iron-binding affinity [29–31]. Three variants show significantly reduced iron affinities, D63S, D63C and G65R [31]. D63S is the ligand mutation found in the C-lobe of melanotransferrin, a naturally occurring mutant found primarily on the surface of melanoma cells [32–35]. Solution X-ray scattering studies suggest that residue Asp-63 is required for the proper closure of the N1 domain over the N2 domain [36]. The substitution D63S apparently prevents the linkage of the domains via the aspartate–iron–carbonate complex and formation of the binding cleft. A second variant D63C was constructed with the goal of possibly altering metal-ion selectivity [30]. The third variant, G65R, mimics the mutation found in the C-terminal

Abbreviations used: hTf, human serum transferrin; hTf/2N, recombinant N-terminal half-molecule of human serum transferrin; OTf, ovotransferrin; LTf, lactoferrin.

‡ To whom correspondence should be addressed.

Table 1 Variants of hTf/2N

Variant	Fe^{3+} ligand changed	Mimic
D63S		
D63C	Yes	Melanotransferrin (C-lobe)
G65R	No	U.K. patient variant (C-lobe)
H207E	No	Lactoferrin (N-lobe)
K206Q	No	Ovotransferrin (C-lobe)
H249Q	Yes	–
H249E	Yes	–
K296E	No	–
K296Q	No	–

lobe of hTf from a patient in the U.K. [37]. The introduction of a positively charged arginine so near the Asp-63 ligand alters binding to the iron [36].

Two other variants, K206Q and H207E, show somewhat enhanced iron affinity [31] and mimic differences between the N-terminal lobe of hTf and either the C-terminal lobe of OTf (K206Q) or the N-terminal lobe of LTf (H207E) (Table 1). This enhanced affinity is consistent with that found for the C-terminal lobe of OTf [38] and the N-terminal lobe of LTf [39]. Both residues Lys-206 and His-207 are found on the interdomain strands of hTf and may influence switching between the open and closed conformational states. The availability of these variants allow us to probe, by EPR spectroscopy, the importance of these residues in the binding of chloride anions without the complicating effects of the presence of a second lobe.

Four more variants have been constructed from changes in residues His-249 and Lys-296 (Table 1). Replacement of the His-249 ligand by either glutamate (H249E) or glutamine (H249Q) may yield clues regarding the importance of the hinge region in iron coordination. Residue Lys-296 has been implicated in the pH-dependent opening of the two domains via an unusual dilysine pair with Lys-206 [40]. These lysines are also potential candidates for chloride binding. Accordingly, Lys-296 was replaced by either glutamate (K296E) or glutamine (K296Q).

In the present study, changes in the Fe^{3+} EPR spectrum as a result of substitution of selected amino acid residues and chloride binding to several variant half-molecules, was investigated. EPR spectra of variants D63S, D63C, G65R, H249E, H249Q, K296E and K296Q were found to be significantly different from that of the wild-type hTf/2N, indicating that alteration of either coordinating or non-coordinating residues can have a pronounced effect on the iron coordination sphere. On the other hand, hTf/2N and the variants K206Q and H207E exhibited a $g' = 4.3$ EPR signal more characteristic of native diferric transferrin. The EPR spectra of all the variants were significantly affected by the presence of NaCl. The results show that Lys-206, Lys-296 and His-207 of the hinge region are not the primary binding sites for Cl^- nor are they the origin of the salt effects on the EPR spectra of the transferrins. Variant G65R appears to be capable of adopting two distinct conformations, one with 'normal' iron coordination in which both domains are closed over the iron and the other an open conformation similar to that found for variants D63S and D63C in which residue 63 is not coordinated to the iron.

MATERIALS AND METHODS

hTf/2N and the nine site-directed variants, D63S, D63C, G65R, H207E, K206Q, H249E, H249Q, K296E and K296Q, were prepared and characterized by procedures previously described [29,30,41]. OTf was isolated from hen egg-white as previously described [42]. The C-terminal lobe of OTf was prepared from diferric OTf by trypsin digestion according to the method of Oe et al. [43]. The N- and C-lobes were almost completely resolved by electrofocusing for approximately 30 h on a large (500 ml) LKB column using 0.4% pH 4–6 ampholytes (Serva, Sevalyt 4-6) in a gradient of 0–50% sucrose. Following collection, the separated lobes were dialysed against cold running water overnight, concentrated on an Amicon stirred cell fitted with a YM-10 membrane, and further purified by chromatography on Sephadex G-75 (1 × 100 cm column) in 100 mM NH_4HCO_3. Final purification was achieved on a Polyanion SI column (Pharmacia) using a linear gradient of NaCl (0–300 mM) in 50 mM Tris-HCl, pH 8.0, over a period of an hour at a flow rate of 1 ml/min.

EPR spectra of frozen solutions were recorded at 77 K using Varian E-4 or E-9 X-band spectrometers outfitted with a liquid nitrogen quartz finger dewar (Wilmad) inserted into the rectangular TE_{102} or TE_{104} cavities respectively. The spectrometers were interfaced to an ISA standard Intel-based 80486 computer using data acquisition and manipulation hardware and EPRWare software purchased from Scientific Software Services, Bloomington, IL, U.S.A.. The protein samples (volume = 350 or 400 μl) were loaded into 4 mm outer diameter, 3 mm internal diameter standardized quartz EPR tubes and frozen. NaCl titrations were performed on the same sample by adding successive microlitre aliquots of 5 M NaCl to the thawed protein solution, initially 0.1 M Hepes/0.01 M sodium bicarbonate, pH 7.5. The spectral intensities were corrected for dilution with a maximum correction of 24.3%. Double integrations of the spectra over the field range 600–2450 G ($1G = 10^{-4}$ T) were performed to ensure that no iron was lost from any of the proteins during the course of the experiment. A series of difference spectra were obtained by subtracting the spectrum of each of the dilution-corrected NaCl-titrated samples from the spectrum in the absence of added NaCl.

The UV/visible spectrum of variants FeH249E, FeH249Q, FeK296E and FeK296Q were measured between 260 and 500 nm on a Cary 219 spectrophotometer. In order to remove any non-specifically bound iron chelates that may be present, these samples were dialysed three times against 0.1 M $NaClO_4$/5 mM Hepes, pH 8.0 (volume ratio 1:1000), followed by exhaustive dialysis against 5 mM Hepes, pH 7.5 [44]. The final dialysis step was performed using 0.1 M Hepes/0.01 M sodium bicarbonate, pH 7.4.

RESULTS

Spectral properties of the variants

The transferrins exhibit a characteristic three-component EPR signal near $g' = 4.3$ (150 mT), flanked by exceptionally broad tails, as shown in spectrum (a) of Figure 1. This spectrum and the others in Figure 1 are described by the spin Hamiltonian

$$\mathcal{H} = g\beta B\cdot\hat{S} + D[\hat{S}_z^2 - S(S+1)/3] + E[\hat{S}_x^2 - \hat{S}_y^2] \quad (1)$$

where $S = 5/2$, $g = 2$ is the electron g factor, β is the Bohr magneton, D and E are the axial and rhombic zero-field splitting constants respectively, B is the applied magnetic field and the $\hat{S}_i$

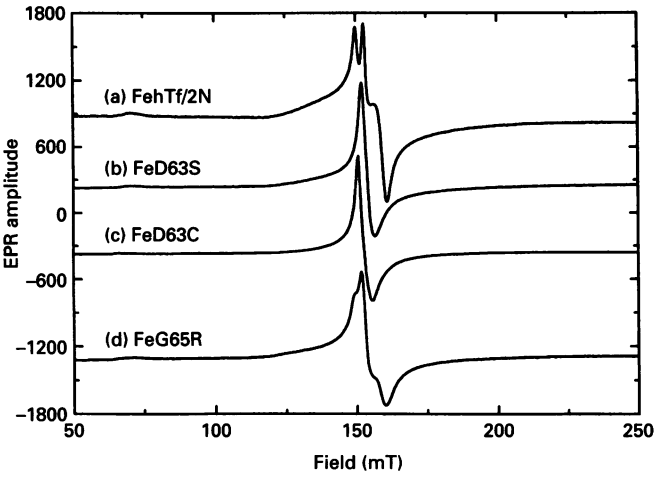

Figure 1 EPR spectra of hTf/2N and various site-directed variants directly affecting the iron site

(a) FehTf/2N, ~ 25 mg/ml; (b) FeD63S, ~ 25 mg/ml; (c) FeD63C, ~ 25 mg/ml; (d) FeG65R, ~ 27.5 mg/ml. Solution conditions: 0.1 M Hepes/0.01 M sodium bicarbonate, pH 7.4. Spectrometer parameters (a)–(d): field set, 1500 G; scan range, 2000 G; power, 20 mW; modulation amplitude, 10 G; time constant, 0.3 s; scan time, 8 min; temperature, 77 K. (a) Gain = 620, frequency = 9.372085 GHz; (b) gain = 400, frequency = 9.372720 GHz; (c) gain = 250, frequency = 9.372747 GHz; (d) gain = 400, frequency = 9.371027 GHz.

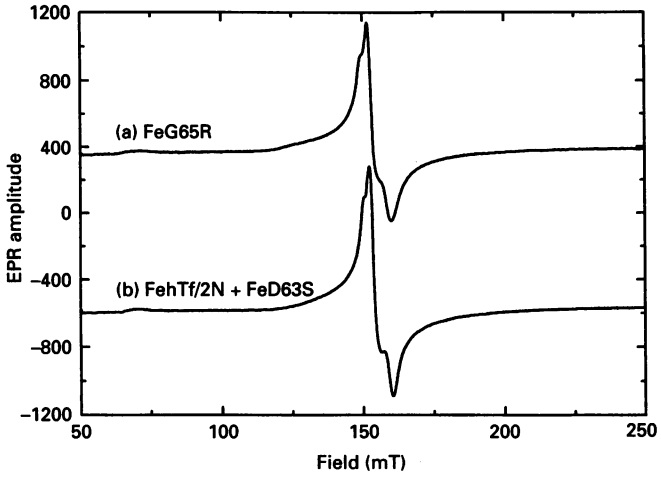

Figure 2 Comparison of the observed EPR spectrum of FeG65R with the spectrum of the equally weighted sum of FehTf/2N and FeD63S

(a) FeG65R, (b) equally weighted sum of FehTf/2N and FeD63S. Solution conditions and spectrometer parameters are the same as in Figure 1.

(i = x,y,z) are the operators for electron spin angular momentum [15,45–47]. The features at $g' = 4.3$ arise primarily from transitions within the middle Kramer's doublet ($3 \rightarrow 4$) of the $S = 5/2$ manifold of spin states. For the case of pure rhombic symmetry, i.e. $E/D = 1/3$, the $g' = 4.3$ resonance is isotropic and lacks structural features [15,45–47]. For small deviations from rhombic symmetry toward axial symmetry ($E/D \lesssim 1/3$), fine structure features begin to appear. Larger deviations in E/D from 1/3 as the ligand field symmetry becomes more axial produce features at lower field near $g' = 6$.

For the high-spin Fe^{3+} metal ion of transferrin, EPR and Mössbauer spectra have shown that $D = 0.25\ cm^{-1}$ and $E/D \sim 1/3$, corresponding to nearly complete rhombic zero-field symmetry [15,46–49]. The observation of three features near $g' = 4.3$ in spectrum (a) of Figure 1 reflects the presence of a small amount of axial character in the ligand field of the Fe^{3+}. Simulation of the entire spectrum, including the broad tailing regions, requires employing a distribution of E/D values for the remaining components of the sample [15,46]. It has been shown that relatively small changes in the E/D ratio can have a pronounced effect on the observed $g' = 4.3$ EPR signal [45,46].

Figure 1 compares the native EPR spectra of the hTf/2N with those of variants with amino acid substitutions at or near the iron ligand Asp-63. While the spectrum of the wild-type half molecule, FehTf/2N, is typical of the transferrins (spectrum a), replacement of Asp-63 by serine or cysteine causes the spectrum to change from slightly axial (spectrum a) to purely rhombic, $E/D = 1/3$ (spectra b and c). The fact that the spectra of D63S and D63C are the same suggests identical coordination about the iron in both variants, namely in neither instance does residue 63 remain a ligand. In variant D63C, residue Cys-63 is cysteinylated with free cysteine and therefore cannot be a ligand to the Fe^{3+} [30].

The spectrum of variant FeG65R is also shown in Figure 1 (spectrum d) and appears to be due to a mixture of species.

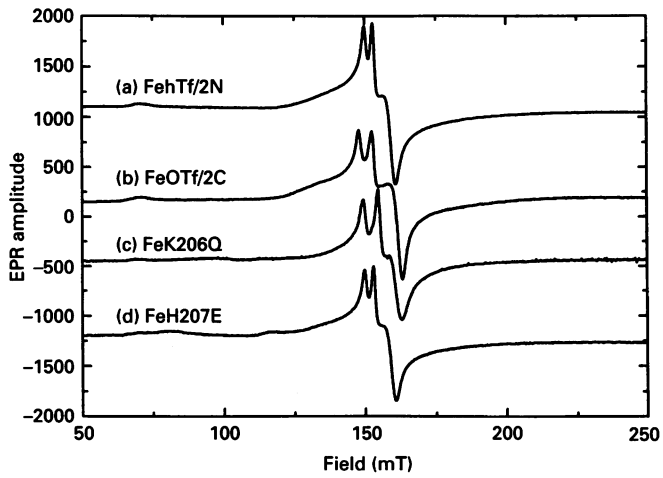

Figure 3 Spectra of various half-molecules with substitutions indirectly affecting the iron site

(a) FehTf/2N, ~ 25 mg/ml; (b) FeOTf/2C proteolytic fragment of OTf, ~ 25 mg/ml; (c) FeK206Q, ~ 21 mg/ml; (d) FeH207E, ~ 27.5 mg/ml. The solution conditions are the same as in Figure 1. Spectrometer parameters: as in Figure 1, except (b) gain = 800, frequency = 9.371960 GHz; (c) gain = 800; frequency = 9.372819 GHz; (d) gain = 1000; frequency = 9.370850 GHz.

Figure 2 compares the spectrum of FeG65R with the calculated sum of the spectra of FehTf/2N and FeD63C weighted equally. The computed spectrum is remarkably close to the experimental spectrum of FeG65R. Although other explanations are possible, this result suggests that variant FeG65R exists in open and closed conformations of equal populations, with the closed conformation exhibiting a 'normal' transferrin spectrum (e.g. Figure 1, spectrum a) and the open conformation exhibiting a spectrum like variant FeD63S or FeD63C in which residue 63 is not a ligand (e.g. Figure 1, spectra b and c).

The EPR spectra of several other half-molecules are presented in Figures 3 and 4. Figure 3 compares the spectra of FehTf/2N

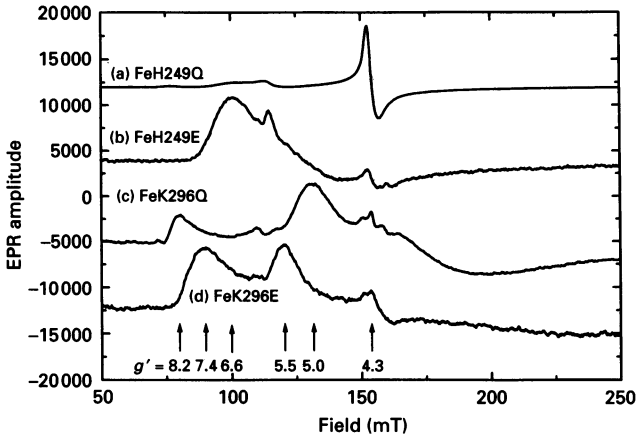

Figure 4 EPR spectra of variants FeH249E, FeH249Q, FeK296Q and FeK296E

(a) FeH249Q, ~ 76 mg/ml; (b) FeH249E, ~ 27 mg/ml; (c) FeK296Q, ~ 20 mg/ml; (d) FeK296E, ~ 38 mg/ml. Solution conditions as in Figure 1. Spectrometer conditions: as in Figure 1, except time constant = 1 s and, (a) gain = 2500, frequency = 9.250759 GHz; (b) gain = 2500, frequency = 9.251196 GHz; (c) gain = 4000, frequency = 9.24991 GHz; (d) gain = 4000, frequency = 9.25630 GHz.

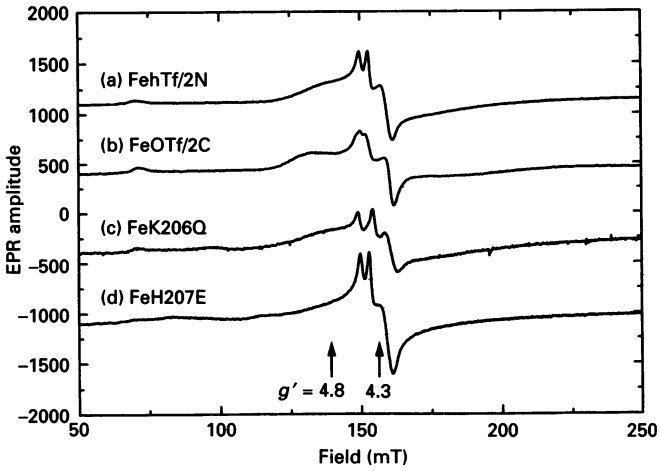

Figure 5 Effect of addition of 0.5 M NaCl to several half-molecules

(a) FehTf/2N, ~ 25 mg/ml; (b) FeOTf/2C proteolytic fragment of OTf, ~ 25 mg/ml; (c) FeK206Q, ~ 21 mg/ml; (d) FeH207E, ~ 27.5 mg/ml. Solution conditions as in Figure 1, except 43.4 μl of 5 M NaCl was added to each 400 μl sample. Spectrometer parameters as in Figure 3, except (a) frequency = 9.370880 GHz; (b) frequency = 9.372240 GHz; (c) gain = 1250, frequency = 9.373443 GHz; (d) frequency = 9.370820 GHz.

and FeOTf/2C (the C-terminal half-molecule of OTf obtained from the proteolytic digestion of OTf) with the spectra of variants FeK206Q and FeH207E. Substitution K206Q makes the signal slightly more axial in character, as evidenced by the increased field spread in the three components of the $g' = 4.3$ signal (cf. spectra a and c). The spread in fine-structure features of this variant more closely resembles that of FeOTf/2C half-molecule which it is intended to mimic (cf. spectra b and c). However, it does not exhibit the small shoulder on the low-field side of the $g' = 4.3$ signal that is characteristic of the ovotransferrins FeOTf/2C (spectrum b). Substitution H207E found in LTf changes the spectrum little from that of the wild-type FehTf/2N (cf. spectra a and d) and so this substitution does not explain the small differences in the EPR spectra between hTf and LTf [50].

The spectra of the His-249 and Lys-296 variants are shown in Figure 4. These substitutions produce the most pronounced spectral changes. Substitution H249Q results in a more rhombic spectrum with a small amount of a protein component with axial character near $g \sim 6$ (spectrum a). In contrast, the substitution of a glutamate at position 249 in FeH249E results in a largely axial spectrum (spectrum b) with $E/D \leqslant 0.1$ as judged from published simulations [15,46,47]. The rhombic signal at $g' = 4.3$ in spectrum (b) is nearly absent, with the majority of the broad EPR signal near $g \sim 6$. The spectra of FeK296E and FeK296Q are also axial in nature and from the work of Seidel et al. [51] and Doctor et al. [47] we estimate $E/D \sim 0.05$–0.10 and $D = 0.25$–0.60. They show a marked loss of the rhombic signal at $g' = 4.3$ (spectra c and d) and are reminiscent of the spectra of the native protein with oxalate substituted for carbonate as the synergistic anion [47,52,53]. The bulk of the intensity is in the low-field region, between $g \sim 5.0$ and $g \sim 8.2$.

All four of the His-249 and Lys-296 variants show 1:1 Fe binding stoichiometries, and UV/vis spectral properties and molar absorptivities very similar to those seen with FehTf/2N (results not shown), indicating that specific iron–protein complexes are formed in all four variants even though they exhibit unusual EPR spectra (Figure 4). The small peaks in the various

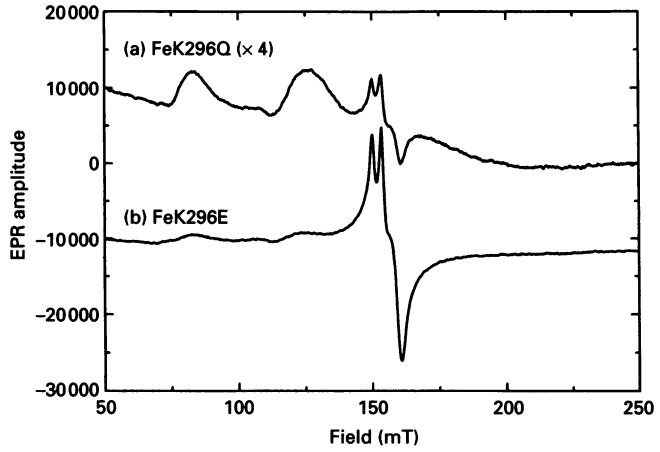

Figure 6 Effect of 0.8 M NaCl addition to variants of Lys-296

(a) FeK296Q, ~ 20 mg/ml; (b) FeK296E, ~ 38 mg/ml. Solution conditions as in Figure 1 except 64.9 μl of 5 M NaCl added to each 350 μl sample. Spectrometer parameters as in Figure 1, except, (a) gain = 4000, frequency = 9.250006 GHz; (b) gain = 1000, frequency = 9.250049 GHz.

spectra of Figure 4 appear to be due to subpopulations of the iron–protein complexes since they are retained after exhaustive dialysis against $NaClO_4$ and change in response to the addition of NaCl to the sample (see below).

Salt effects

The effect of the addition of 0.5 M NaCl on the EPR spectrum of the wild-type and five variant proteins is shown in Figures 5 and 6. In Figure 5 the EPR amplitude at $g' = 4.3$ is reduced and a characteristic shoulder at $g' \approx 4.77$–4.91 develops in the presence of salt, indicative of increased axial character in the spectra of these proteins. For the wild-type half-molecule, FehTf/2N, the shoulder is quite pronounced and the EPR

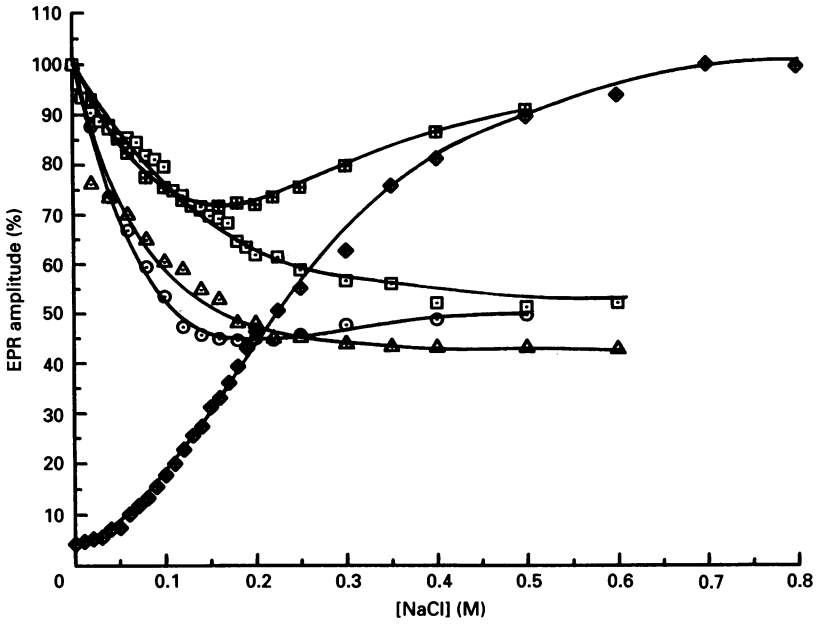

Figure 7 Change in EPR peak-to-peak amplitude as a function of NaCl concentration

(⊙) FehTf/2N, ~ 25 mg/ml; (⊞) FeH207E, ~ 27.5 mg/ml; (△) FeK206Q, ~ 21 mg/ml; (⊡) Fe_2hTf, ~ 76 mg/ml; (◇) FeK296E, ~ 38 mg/ml. Amplitudes were corrected for dilution.

amplitude is reduced relative to that of the native sample (cf. Figures 1 and 5, spectrum a). Double integration of the spectra of the various samples indicated that the EPR spectrum quantitatively accounted for all the iron present within ±10%.

The spectrum of the C-terminal OTf fragment, FeOTF/2C, is also markedly affected by the presence of NaCl (cf. Figures 3 and 5, spectrum b). The $g' \approx 4.8$ shoulder is quite pronounced, the doublet feature near $g' = 4.3$ becomes poorly resolved and the amplitude significantly reduced compared with the sample without NaCl. Similarly, the spectrum of FeK206Q develops a pronounced shoulder at $g' \approx 4.8$ with a loss of signal amplitude at $g' = 4.3$ (cf. Figures 3 and 5, spectrum c). However, in contrast to FeOTf/2C (spectrum b), resolution of the doublet at $g' = 4.3$ is still evident in FeK206Q (spectrum c). Variant FeH207E has a much less perturbed EPR signal in the presence of NaCl than the other variants (cf. Figures 3 and 5, spectrum d). The addition of NaCl results in a weak shoulder at $g' \approx 4.8$ and essentially no loss of resolution of the doublet near $g' = 4.3$.

Variants FeK296E and FeK296Q displayed behaviour which was quite different from the other variants upon addition of NaCl (Figure 6). The characteristic $g' = 4.3$ signal of the transferrins, which is nearly absent in the sample without NaCl, (Figure 4, spectra c and d) was restored when 0.8 M NaCl was added (Figure 6, spectra a and b). The increase in $g' = 4.3$ amplitude was most pronounced with the FeK296E variant, being over 20-fold, while the $g' = 4.3$ signal of FeK296Q increased by ~ 3.5-fold at 0.8 M NaCl.

To ascertain the binding properties of Cl^- and the effects of salts in general on the spectral properties of these variants, a titration of the iron-loaded half-molecules was performed by adding successive aliquots of 5 M NaCl to the samples. A plot of the change in $g' = 4.3$ EPR amplitude as a function of chloride concentration is shown in Figure 7 for FehTf/2N, FeH207E, FeK206Q, Fe_2hTf and FeK296E. For the first four samples a reduction in the EPR amplitude is observed which is essentially complete at an NaCl concentration near 0.16 M, the physiological chloride concentration. This reduction is presumably associated with a conformational change in the protein as previously proposed [18,44]. Curiously, for FeH207E, the amplitude of the $g' = 4.3$ signal decreases and then increases with increased salt concentration (Figure 7), suggesting a further conformational change at high salt concentration. FehTf/2N shows somewhat similar behaviour but to a lesser extent (Figure 7). In contrast, as NaCl is added to variants FeK296E (Figure 7) and FeK296Q (not shown), the $g' = 4.3$ signal increases at the expense of the $g' = 7.35$ and $g' = 5.48$ features in the spectrum (cf. Figures 4 and 6).

Figure 8 shows the spectra of FehTf/2N with and without NaCl (spectra a and b) and the difference spectrum (spectrum c). The variation in the amplitude, h, of the difference spectrum as a function of NaCl concentration approximately follows a saturation binding isotherm (Figure 7). Attempts were made to model the data according to the following simple equilibrium as done previously for anion binding to diferric and monoferric transferrins [18].

$$\text{Fe-lobe} + n\text{Cl}^- \rightleftharpoons \text{Fe-lobe–Cl}_n \quad (2)$$

Here n chloride ions bind cooperatively to the Fe-lobe of the half-molecule. Fe-lobe exhibits the EPR spectrum of the native protein (Figure 8, spectrum a) and the species Fe-lobe–Cl_n is assumed to exhibit the perturbed spectrum of the new conformation in the presence of NaCl (e.g. Figure 8, spectrum b). The equilibrium constant is given by

$$K = \frac{[\text{Fe-lobe–Cl}_n]}{[\text{Fe-lobe}][\text{Cl}^-]^n} = \frac{\Theta}{(1-\Theta)[\text{Cl}^-]^n} \quad (3)$$

where Θ, the degree of saturation of the binding sites, is given by $\Theta = h/h_{max.}$. $h_{max.}$ is the maximum height of the EPR difference spectrum, namely the value of h at saturation of the binding sites. The corresponding Hill equation is given by

$$-\text{Log}[\Theta/(1-\Theta)] = -n\log[\text{Cl}^-] - \log K \quad (4)$$

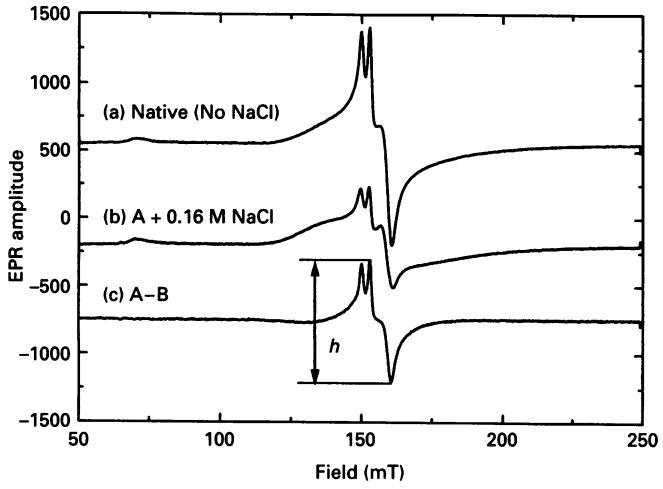

Figure 8 Typical subtraction spectrum used for determination of loss of the signal at $g' = 4.3$

(a) Native FehTf/2N; (b) +0.16 M NaCl FehTf/2N; (c) difference spectrum = spectrum (a) − spectrum (b).

which predicts a straight line with a slope of n, the number of chloride ions, and an intercept $-\log K$.

The results of the Hill analysis for some of the proteins are shown in Figure 9. All of the Hill plots show pronounced curvature, indicating that the simple cooperative binding model does not adequately describe these data. The spectrum for variant FeK296E is similar to those of the other variants even though its $g' = 4.3$ signal increases rather than decreases with added salt (Figure 7). Experiments repeated for diferric serum transferrin likewise showed modest curvature (Figure 9) not seen in earlier work [18].

Attempts were made to account for the curvature in the Hill plots by analysing the data using a more sophisticated equilibrium model including stepwise binding of Cl^- anions. Satisfactory fits were still not obtained. Even Na_2SO_4, which is lower on the lyotropic series than most anions [54], has no effect on the line-shape or appearance of the EPR spectrum but nevertheless causes a reduction and then a recovery in the $g' = 4.3$ EPR signal of Fe_2hTf (results not shown).

DISCUSSION

All of the single point mutations which were made affect the iron-binding site of transferrin either directly or indirectly, as reflected by changes in the EPR spectrum when coordinating or non-coordinating ligands are replaced (Figures 1, 3 and 4). The EPR spectra of the D63S, D63C, G65R, H249E and H249Q variants demonstrate that the iron coordination in these proteins is markedly different from that in the native protein (Figures 1 and 4) as expected, since the ligation to the iron has been changed. The loss of residue Asp-63 as a ligand results in identical spectra for the variants D63S and D63C, which are similar to the pure rhombic spectra seen for simple iron-chelates of low symmetry [55–58]. Recent calorimetric and X-ray scattering studies have demonstrated the importance of Asp-63 ligation for proper closing of the N1 domain to form the binding cleft for Fe^{3+} [30,31,36].

The addition of a positively charged arginine residue only two positions away from the Asp-63 ligand in variant G65R results in reduced affinity for Fe^{3+} compared with the wild-type FehTf/2N. However, the stability of variant FeG65R (which from the sum of spectra in Figure 2 appears to exist in an equilibrium mixture of open, with the loss of Asp-63 as a ligand,

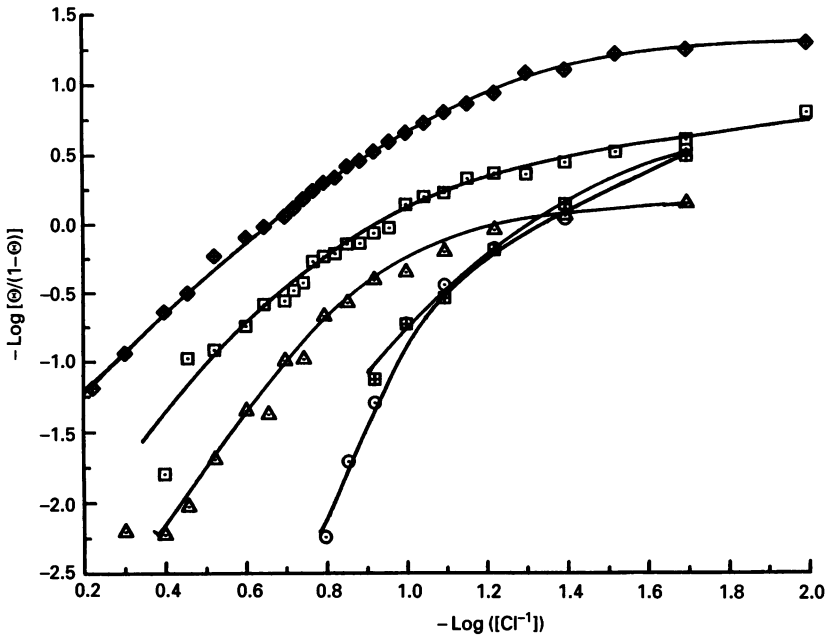

Figure 9 Hill plots of the half-molecules

(○) FehTf/2N; (⊞) FeH207E; (△) FeK206Q; (□) Fe_2hTf; (◇) FeK296E. Solution conditions are given in Figure 7.

and closed conformations) is still ~ 10-fold higher than that of either of the open conformation variants D63S or D63C, indicating that a more stable iron environment is achieved upon domain closure [30,31].

Evans and Madden [59] reported that the C-terminal lobe of the electrophoretically slow variant of hTf, which the variant G65R is intended to mimic, exhibits a spectrum nearly identical with that seen for an 18 kDa fragment of OTf [59]. This 18 kDa fragment is from the N2 domain of OTf and lacks the aspartic acid from the N1 domain [60]. Therefore, it is expected to exhibit a rhombic-type spectrum similar to the Asp-63 variants and to the open conformation of FeG65R studied here.

The spectra of the FeH249Q and FeH249E variants illustrate the effect of the substitution of an iron ligand from the hinge region. The characteristic three-component $g' = 4.3$ signal of transferrin is lost in both variants. The FeH249Q variant spectrum is largely axial in character whereas the spectrum of variant FeH249E consists of a rhombic $g' = 4.3$ signal, suggesting that the glutamate residue introduced in H249E is probably acting as an iron ligand in this instance. In any event, substitution of the iron ligand His-249 by either glutamate or glutamine, the latter residue being a non-ligand, markedly alters the environment of the iron-binding site.

The Hill analysis of the data for all the half-molecules gave very similar chloride-binding curves (Figure 9), suggesting that the same or similar conformational changes occur in all the variants even though the observed spectral changes are different (cf. Figures 3–6). This result indicates that, while replacement of the hinge region residues Lys-206, His-207 or Lys-296 alters the binding environment of the Fe^{3+}, they cannot be the site of chloride binding responsible for the observed changes in the EPR spectrum.

The similarity in the Hill plots for all the proteins (Figure 9) indicates that the residues involved in the salt effects on the EPR spectra have not been replaced in any of the variants. One possible site of chloride binding is the conserved residue Arg-124 [3]. This residue is involved in coordination to the carbonate and appears to function to 'lock in' the iron within the binding cleft. Binding of chloride to one of the side-chain amino groups could disrupt the hydrogen-bonding between the arginine and carbonate anion, which may then serve to increase the likelihood of domain opening due to a destabilization of the carbonate ligand.

The observation that the maximum amplitude loss occurs near the physiological concentration of NaCl (Figure 7) suggests that the native conformation of the protein has chloride bound to specific sites, consistent with the salt requirement for iron removal from the protein [28]. All salts affect the amplitude of the EPR signal, including Na_2SO_4, which, in contrast to the others, does not change the EPR line-shape. Both anion-binding and ionic strength effects play a role in perturbing the EPR spectrum, since different salts affect the spectral amplitudes and line-shape differently at the same ionic strength [18,20,44,61]. It has thus proven difficult to find a suitable non-interacting salt for use as a background electrolyte when carrying out anion-binding studies.

From the present work it is clear that chloride binding to the transferrins is more complex than previous data indicated [18]. Our inability to adequately fit the EPR data to various binding models underscores both the complexity and sensitivity of the transferrins to chloride binding and to ionic strength. Although the site of chloride binding was not identified by the present work, several possibilities have been eliminated. The results of the present study further emphasize, however, the importance of conformational states in governing the iron binding and release properties of transferrin.

This study was supported by USPHS grants R37 GM20194 (N.D.C.) from the National Institute of General Medical Sciences and R01 DK 21739 (R.C.W.) from the National Institute of Diabetes, and Digestive and Kidney Diseases.

REFERENCES

1 Harris, D. C. and Aisen, P. (1989) in Iron Carriers and Iron Proteins (Loehr, T. M., ed.), pp. 239–351, VCH Publishers, Weinheim
2 Chasteen, N. D. and Woodworth, R. C. (1990) in Iron Transport and Storage (Ponka, P., Schulman, H. M. and Woodworth, R. C., eds.), pp. 67–79, CRC Press, Boca Raton
3 Anderson, B. F., Baker, H. M., Norris, G. E., Rice, D. W. and Baker, E. N. (1989) J. Mol. Biol. **209**, 711–734
4 Anderson, B. F., Baker, H. M., Norris, G. E., Rumball, S. V. and Baker, E. N. (1990) Nature (London) **344**, 784–787
5 Anderson, B. F., Baker, H. M., Dodson, E. J., Norris, G. E., Rumball, S. V., Waters, J. M. and Baker, E. N. (1987) Proc. Natl. Acad. Sci. U.S.A. **84**, 1769–1773
6 Bailey, S., Evans, R. W., Garratt, R. C., Gorinsky, B., Hasnain, S., Horsburgh, C., Jhoti, H., Lindley, P. F., Mydin, A., Sarra, R. and Watson, J. L. (1988) Biochemistry **27**, 5804–5812
7 Schlabach, M. R. and Bates, G. W. (1975) J. Biol. Chem. **250**, 2182–2188
8 Antonini, A., Leenders, K. L., Meier, D., Oertel, W. H., Boesiger, P. and Anliker, M. (1993) Neurology **43**, 697–700
9 Shongwe, M. S., Smith, C. A., Ainscough, E. W., Baker, H. M., Brodie, A. M. and Baker, E. N. (1992) Biochemistry **31**, 4451–4458
10 Zak, O. and Aisen, P. (1990) Biochim. Biophys. Acta **1052**, 24–28
11 Chasteen, N. D. (1977) Coord. Chem. Rev. **22**, 1–36
12 Baldwin, D. A. (1980) Biochim. Biophys. Acta **623**, 183–198
13 Zak, O. and Aisen, P. (1988) Biochemistry **27**, 1075–1080
14 Baldwin, D. A. and Egan, T. J. (1987) S. African J. Sci. **83**, 22–31
15 Gaffney, B. G. and Silverstone, H. J. (1993) Biol. Magn. Reson. **13**, 1–57
16 Smith, C. A., Anderson, B. F., Baker, H. M. and Baker, E. N. (1992) Biochemistry **31**, 4527–4533
17 Day, C. L., Anderson, B. F., Tweedie, J. W. and Baker, E. N. (1993) J. Mol. Biol. **232**, 1084–1100
18 Folajtar, D. A. and Chasteen, N. D. (1982) J. Am. Chem. Soc. **104**, 5775–5780
19 Chasteen, N. D., Thompson, C. P. and Rines, J. P. (1983) in Structure and Function of Iron Storage and Transport Proteins (Urushizaki, I., ed.), pp. 241–246, Elsevier Science Publishers B. V., Amsterdam
20 Thompson, C. P., McCarty, B. M. and Chasteen, N. D. (1986) Biochim. Biophys. Acta **870**, 530–537
21 Bertini, I., Hirose, J., Kozlowski, H., Luchinat, C., Messori, L. and Scozzafava, A. (1988) Inorg. Chem. **27**, 1081–1086
22 Williams, J., Chasteen, N. D. and Moreton, K. (1982) Biochem. J. **201**, 527–532
23 Baldwin, D. A. and de Sousa, D. M. R. (1981) Biochem. Biophys. Res. Commun. **99**, 1101–1107
24 Baldwin, D. A., Egan, T. J. and Marques, H. M. (1990) Biochim. Biophys. Acta **1038**, 1–9
25 Egan, T. J., Ross, D. C., Purves, L. R. and Adams, P. A. (1992) Inorg. Chem. **31**, 1994–1998
26 Egan, T. J., Zak, O. and Aisen, P. (1993) Biochemistry **32**, 8162–8167
27 Chasteen, N. D., Grady, J. K., Woodworth, R. C. and Mason, A. B. (1993) in Lactoferrin: Structure and Function (Hutchens, T. W., Lonnerdal, B. and Rumball, S. V., eds.), pp. 1–8, Plenum Press, New York
28 Kretchmar, S. A. and Raymond, K. N. (1988) Inorg. Chem. **27**, 1436–1441
29 Funk, W. D., MacGillivray, R. T. A., Mason, A. B., Brown, S. A. and Woodworth, R. C. (1990) Biochemistry **29**, 1654–1660
30 Woodworth, R. C., Mason, A. B., Funk, W. D. and MacGillivray, R. T. A. (1991) Biochemistry **30**, 10824–10829
31 Lin, L. N., Mason, A. B., Woodworth, R. C. and Brandts, J. F. (1993) Biochem. J. **293**, 517–522
32 Richardson, D. R. and Baker, E. (1991) Biochim. Biophys. Acta **1053**, 1–12
33 Rose, T. M., Plowman, G. D., Teplow, D. B., Dreyer, W. J., Hellstrom, K. E. and Brown, J. P. (1986) Proc. Natl. Acad. Sci. U.S.A. **83**, 1261–1265
34 Brown, J. P., Woodbury, R. G., Hart, C. E., Hellstrom, I. and Hellstrom, K. E. (1981) Proc. Natl. Acad. Sci. U.S.A. **78**, 539–543
35 Baker, E. N., Baker, H. M., Smith, C. A., Stebbins, M. R., Kahn, M., Hellstroem, K. E. and Hellstroem, I. (1992) FEBS Lett. **298**, 215–218
36 Grossmann, J. G., Mason, A. B., Woodworth, R. C., Neu, M., Lindley, P. F. and Hasnain, S. S. (1993) J. Mol. Biol. **231**, 554–558
37 Evans, R. W., Williams, J. and Moreton, K. (1982) Biochem. J. **201**, 19–26
38 Ulundu, L. S. (1989) Ph.D. Thesis, University of Vermont, Burlington
39 Harris, W. R. (1989) Adv. Exp. Med. Biol. **249**, 67–93
40 Dewan, J. C., Mikami, B., Hirose, M. and Sacchettini, J. C. (1993) Biochemistry **32**, 11963–11968

41 Mason, A. B., Funk, W. D., MacGillivray, R. T. A. and Woodworth, R. C. (1991) Protein Expression Purif. **2**, 214–220
42 Mason, A. B., Brown, S. A., Butcher, N. D. and Woodworth, R. C. (1987) Biochem. J. **245**, 103–109
43 Oe, H., Doi, E. and Hirose, M. (1988) J. Biochem. (Tokyo) **103**, 1066–1072
44 Price, E. M. and Gibson, J. F. (1972) J. Biol. Chem. **247**, 8031–8035
45 Scullane, M. I., White, L. K. and Chasteen, N. D. (1982) J. Magn. Reson. **47**, 383–397
46 Yang, A. S. and Gaffney, B. J. (1987) Biophys. J. **51**, 55–67
47 Doctor, K. S., Gaffney, B. J., Alvarez, G. and Silverstone, H. J. (1993) J. Phys. Chem. **97**, 3028–3033
48 Spartalian, K., Lang, G. and Woodworth, R. C. (1991) Biochemistry **30**, 1004–1009
49 Kretchmar, S. A., Teixeira, M., Huynh, B. H. and Raymond, K. N. (1988) Biol. Metals **1**, 26–32
50 Aisen, P. (1973) in Inorganic Biochemistry (Eichhorn, G. L., ed.), pp. 280–304, Elsevier Scientific Publishing Co., New York
51 Seidel, A., Bill, E., Haeggstroem, L., Nordblad, P. and Kilar, F. (1994) Arch. Biochem. Biophys. **308**, 52–63
52 Najarian, R. C., Harris, D. C. and Aisen, P. (1978) J. Biol. Chem. **253**, 38–42
53 Dubach, J., Gaffney, B. J., More, K., Eaton, G. R. and Eaton, S. S. (1991) Biophys. J. **59**, 1091–1100
54 Record, T. M., Jr., Anderson, C. F. and Lohman, T. M. (1978) Q. Rev. Biophys. **2**, 103
55 Mansour, A. N., Thompson, C. P., Theil, E. C., Chasteen, N. D. and Sayers, D. E. (1985) J. Biol. Chem. **260**, 7975–7979
56 Ecker, D. J., Lancaster, J. R., Jr. and Emery, T. (1982) J. Biol. Chem. **257**, 8623–8626
57 Lang, G., Aasa, R., Garbett, K. and Williams, R. J. P. (1971) J. Phys. Chem. **55**, 4539–4548
58 Oosterhuis, W. T. (1974) in Structure and Bonding (Dunitz, J. D., Hemmerich, P., Holm, R. H., Ibers, J. A., Jorgensen, C. K., Neilands, J. B., Reinen, D. and Williams, R. J. P., eds.), pp. 59–99, Springer–Verlag, New York/Heidelberg/Berlin
59 Evans, R. W. and Madden, A. D. (1984) Biochem. Soc. Trans. **12**, 661–662
60 Lindley, P. F., Bajaj, M., Evans, R. W., Garratt, R. C., Hasnain, S. S., Jhoti, H., Kuser, P., Neu, M., Patel, K. and Sarra, R. (1993) Acta Crystallogr. Sect. D. Biol. Crystallogr. **D49**, 292–304
61 Folajtar, D. A. and Chasteen, N. D. (1982) in The Biochemistry and Physiology of Iron (Saltman, P. and Hegenauer, J., eds.), pp. 35–41, Elsevier North Holland Inc., New York/Amsterdam/Oxford

Received 8 December 1994/20 February 1995; accepted 6 March 1995